3.3 Strongly Correlated Quantum Systems

Numerical Studies on Finite-Temperature Properties of Superconductivity in Cuprates

Dai Kubota, Kota Ido, Kensaku Takai, Huihai Zhao, Yusuke Nomura,
Takahiro Ohgoe, and Masatoshi Imada
Department of Applied Physics, University of Tokyo
Hongo 7-3-1, Bunkyo-ku, Tokyo 113-8656

Superconductivity in cuprates has attracted extensive attention since its discovery. In bulk, the discovery of (short-ranged) charge order has raised renewed interest in the relationship between pseudogap and superconductivity [1]. At interfaces, several exotic phenomena which are not observed in the bulk has been reported. For example, at the interface of La_2CuO_4 (insulator) and $La_{2-x}Sr_xCuO_4$ (metal), it has been shown that the transition temperature (T_c) of the interface superconductivity is anomalously pinned around the maximum T_c in bulk (~ 42 K) irrespective of doping concentration x in the metallic layers [2].

As for the interfaces, a previous study using high-accuracy many-variable variational Monte Carlo (mVMC) method [3] has given an explanation for the anomalous behavior of T_c at interfaces [4]. This study has revealed that the doping concentration at the interface is self-optimized to the optimal doping by the interlayer phase separation, which leads to the pinned superconducting order parameter at zero temperature. The pinned superconducting order parameter at $T = 0$ naturally explains the pinning of T_c.

The interlayer phase separation is realized to avoid the charge inhomogeneity within the layer. The instability for intralayer phase separation or charge inhomogeneity in bulk has been suggested by the mVMC calculations at $T = 0$. It has also revealed that the phase separation and associated uniform charge fluctuations play an important role in realizing high T_c superconductivity [5]. However, to discuss the relationship between charge instability and T_c, it is advantageous to perform finite-temperature calculations which can directly calculate T_c. It is also an important problem to investigate whether the instability for the phase separation persists to finite temperatures. Therefore, in this project, we extend the study to finite temperatures and investigate the microscopic origin for charge instability and the role of charge fluctuations in the superconductivity.

For this purpose, we study multi-layer Hubbard model defined as

$$\begin{aligned} H = &-t \sum_{\langle i,j\rangle,\nu,\sigma} (c^\dagger_{i\nu\sigma} c_{j\nu\sigma} + \text{h.c.}) \\ &- t_z \sum_{i,\sigma,\langle\nu,\nu'\rangle} (c^\dagger_{i\nu\sigma} c_{i\nu'\sigma} + \text{h.c.}) \\ &+ U \sum_{i,\nu} n_{i\nu\uparrow} n_{i\nu\downarrow} - \sum_{i\nu} \epsilon_\nu n_{i\nu}, \end{aligned} \tag{1}$$

where $c_{i\nu\sigma}$ ($c^\dagger_{i\nu\sigma}$) is an annihilation (creation) operator of an electron with spin σ at ith site on νth layer. The number operators are defined as $n_{i\nu\sigma} = c^\dagger_{i\nu\sigma} c_{i\nu\sigma}$, and $n_{i\nu} = n_{i\nu\uparrow} + n_{i\nu\downarrow}$. The chemical potential ϵ_ν can be layer-dependent in the simulation for interfaces. t (t_z) is the intralayer (interlayer) transfer. The onsite Coulomb interaction U is set to $U = 8t$.

We apply the cellular dynamical mean field theory (CDMFT) [6] to this model. In the cDMFT, we solve the cluster impurity problem

embedded in self-consistently determined bath sites. The impurity problem is analyzed by exact diagonalization method extended to finite temperatures [7]. As a result, we have obtained several solutions: d-wave superconductivity (d-SC), antiferromagnetic (AF) phase, and the coexistence between d-SC and AF. We have calculated the grand canonical potential for these phases and found that there exists instability for phase separation also at finite temperature. If we make interfaces, this intralayer phase separation will be avoided by the interlayer phase separation, and the stable interface superconductivity will emerge.

It will also be interesting to perform finite-temperature calculations using the mVMC. We have already formulated finite-temperature variational Monte Carlo (FT-VMC) scheme [8]. Combining mVMC with the tensor-network will further improve the accuracy [9]. Studies in this direction is under way.

References

[1] G. Ghiringhelli *et al.*, Science **337**, 821 (2012); J. Chang *et al.*, Nat. Phys. **8**, 871 (2012).

[2] J. Wu *et al.*, Nat. Mater. **12**, 877 (2013).

[3] D. Tahara and M. Imada, J. Phys. Soc. Jpn. **77**, 114701 (2008).

[4] T. Misawa *et al.*, Sci. Adv. **2**, e1600664 (2016).

[5] T. Misawa and M. Imada, Phys. Rev. B **90**, 115137 (2014).

[6] A. I. Lichtenstein and M. I. Katsnelson, Phys. Rev. B **62**, R9283 (2000); G. Kotliar *et al.*, Phys. Rev. Lett. **87**, 186401 (2001).

[7] S. Sakai *et al.*, Phys. Rev. Lett. **116**, 057003 (2016).

[8] K. Takai *et al.*, J. Phys. Soc. Jpn. **85**, 034601 (2016).

[9] H.-H. Zhao *et al.*, arXiv:1703.03537.

Creation and Control of Skyrmions with Different Topological Numbers in Itinerant Magnets

Ryo Ozawa, Yasuyuki Kato, and Yukitoshi Motome
Department of Applied Physics, University of Tokyo 113-8656 Hongo, Bunkyo-Ku, Tokyo

A magnetic Skyrmion, which is a swirling noncoplanar spin texture, has been intensively studied not only from the viewpoint of fundamental physics but also for potential applications to magnetic devices, mainly owing to the robustness protected by the topological nature. Most of previous studies thus far have been concerned primarily with the Skyrmions with topological number of one ($n_{\rm sk} = 1$). For further extensions of potential applications, other types of Skyrmions have been desired, both experimentally and theoretically.

In this study, we explore a new type of Skyrmions in a fundamental model for itinerant magnets by large-scale simulation. We here focus on the stabilization mechanism not by the competition between ferromagnetic and Dzyaloshinskii-Moriya interactions, which has been intensively studied for the conventional Skyrmions with $n_{\rm sk} = 1$, but by the Fermi surface instability, existing ubiquitously in itinerant magnets. Specifically, we study the ground state and finite-temperature properties of the Kondo lattice model on a triangular lattice by a recently-developed efficient algorithm based on both the kernel polynomial method (KPM) and the Langevin dynamics (LD) [1], which we call the KPM-LD simulation. For the KPM-LD simulation, we utilize massive parallel processing by general-purpose computing on graphics processing units (GPGPU) to perform the sparse matrix operations in the KPM. The GPGPU calculations on an ACC node of the system B at ISSP achieve $\sim$350 times faster KPM-LD simulation compared with the CPU calculation on a single core.

We find that a Skyrmion crystal with unusual high topological number $n_{\rm sk} = 2$ is stabilized even without magnetic fields [2]. This is in stark contrast to the Skyrmions in the previous studies, which have $n_{\rm sk} = 1$ and become thermodynamically stable only in nonzero magnetic fields. We also reveal that the Skyrmion crystal state with $n_{\rm sk} = 2$ shows successive phase transitions with multiple digital changes of $n_{\rm sk}$ from two to one, and to zero while increasing an external magnetic field (see Fig. 1).

Furthermore, we find that by raising temperature the topological charge in the Skyrmion crystal with $n_{\rm sk} = 2$ decreases gradually from two to zero. This is also contrast to a rather rapid change in the Skyrmion crystal with $n_{\rm sk} = 1$ [3].

Finally, we emphasis that the large-scale simulations using the massive GPGPU system were crucially important for the finding of this new high-topological-number Skyrmion. This is because the itinerant electron systems are rather sensitive to the finite-size effect in general, and stabilizing the true ground state often fails in small systems. Our results of multiple digital switching of topological number $n_{\rm sk}$ can bring about a great impact on the active fields in spintronics.

References

[1] K. Barros and Y. Kato, Phys. Rev. B **88**, 235101 (2013).

[2] R. Ozawa, S. Hayami, and Y. Motome, Phys. Rev. Lett. **118**, 147205 (2017).

[3] R. Ozawa, Y. Kato, S. Hayami, and Y. Motome, JPS 2017 Annual (72nd) Meeting (19pC24-9).

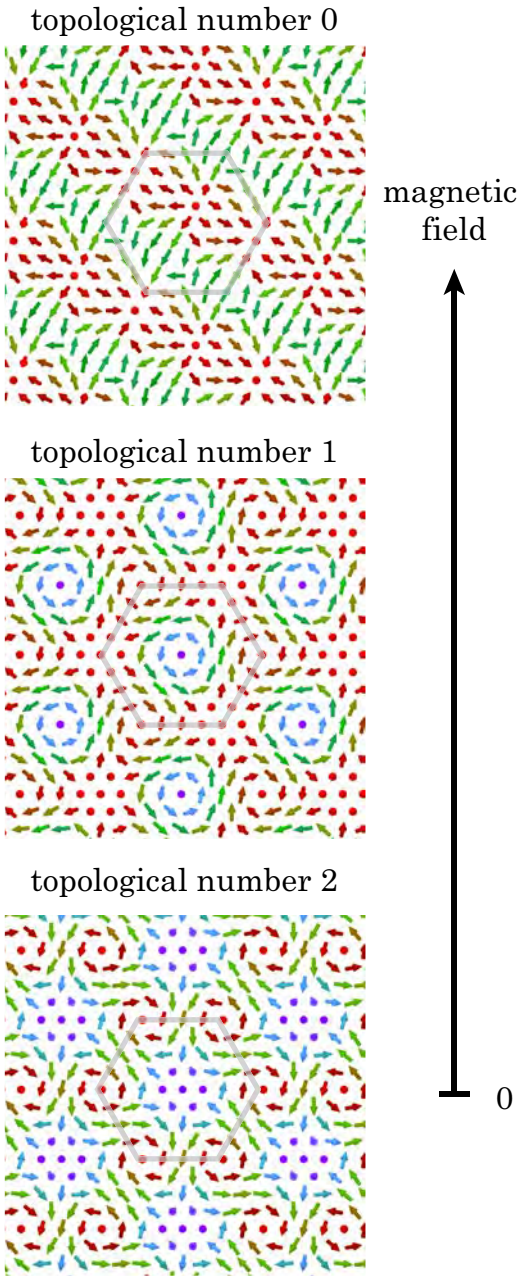

Figure 1: Spin configurations of a $n_{\mathrm{sk}} = 2$ Skyrmion crystal (bottom), a $n_{\mathrm{sk}} = 1$ Skyrmion crystal (middle), a $n_{\mathrm{sk}} = 0$ vortex crystal (top). They are switchable by an external magnetic field.

Theoretical study of novel quantum phenomena in strongly-correlated spin-orbit coupled systems

Yukitoshi MOTOME

Department of Applied Physics,

The University of Tokyo, Bunkyo, Tokyo 277-8581

We have theoretically studied novel quantum phenomena arising from the competition and cooperation between strong electron correlations and spin-orbit coupling. In this project, we have been making substantial progress on the following four topics. We summarize the main achievements for each topic below.

(i) *Spin dynamics, exotic phase transitions, and thermal transport in the Kitaev model*: The Kitaev model, whose ground state is exactly given by a quantum spin liquid with long-range entanglement, is believed to well describe magnetic properties of spin-orbital entangled Mott insulators, such as iridates, ruthenates, and rhodates. For providing theoretical inputs for experiments in these compounds, we have studied the fundamental physics associated with the quantum spin liquid nature in the Kitaev model. Performing the quantum Monte Carlo simulation in a Majorana fermion representation, we obtained the quantitative results for the magnetic Raman scattering [1,2], the temperature and energy dependences of spin dynamics [3-5], an exotic liquid-to-liquid transition by introducing the Ising interaction [6], and thermal transport [7].

(ii) *Vortex crystals, skyrmions, and chiral soliton lattices in spin-charge coupled systems*: Itinerant frustration has been attracted much attention as a source of noncollinear and noncoplanar spin textures. We have explored such spin textures in a fundamental model for itinerant magnets, the Kondo lattice model. Performing large-scale Langevin dynamics simulation with the kernel polynomial method and variational calculations, we discovered a vortex crystal state as a generic ground state in the weak coupling limit [8], a skyrmion crystal with a high topological number [9,10], and collinear multiple-Q states [11]. We constructed an effective model for understanding of the stabilization mechanism [12]. We also studied the magnetotransport in a chiral soliton lattice by quantum Monte Carlo simulation [13].

(iii) *Nonreciprocal and off-diagonal responses in spontaneously parity broken systems*: The spin-orbit coupling brings about rich phenomena, in particular, in the system with spatial inversion symmetry breaking. We have studied nonreciprocal and off-diagonal responses in such systems. We clarified that

asymmetric magnon excitations arise with an antiferromagnetic ordering on a zigzag chain [15]. We summarized a review type article on this topic [16]. We also studied multiferroic properties in a compound composed with low-symmetric square cupolas of Cu $S = 1/2$ spins in collaboration with experimental groups [17].

(iv) *ab initio study of atomically-thin materials with strong spin-orbit coupling*: To further explore intriguing phenomena by the spin-orbital entanglement, we have initiated a project on the basis of *ab initio* calculations supplemented by model analyses. Studying a family of the monolayer form of transition metal trichalcogenides, we predicted that the compounds will show peculiar multiple Dirac cones near the Fermi level due to the lattice geometry and orbital anisotropy. Furthermore, we found that they become topologically nontrivial magnets by electron correlation and carrier doping [18].

References

[1] J. Nasu, J. Knolle, D. L. Kovrizhin, Y. Motome, and R. Moessner: Nature Physics **12** (2016) 912.

[2] 東京大学大学院工学系研究科 プレスリリース (2016.07.05 付)

[3] J. Yoshitake, J. Nasu, and Y. Motome: Phys. Rev. Lett. **117** (2016) 157203.

[4] J. Yoshitake, J. Nasu, Y. Kato, and Y. Motome: preprint (arXiv:1704.02707).

[5] S.-H. Do, S.-Y. Park, J. Yoshitake, J. Nasu, Y. Motome, Y. S. Kwon, D. T. Adroja, D. J. Voneshen, K. Kim, T.-H. Jang, J.-H. Park, K.-Y. Choi, and S. Ji: preprint (arXiv:1703.01081).

[6] J. Nasu, Y. Kato, J. Yoshitake, Y. Kamiya, and Y. Motome: Phys. Rev. Lett. **118** (2017) 137203.

[7] J. Nasu, J. Yoshitake and Y. Motome: preprint (arXiv:1703.10395).

[8] R. Ozawa, S. Hayami, K. Barros, G-W. Chern, Y. Motome, and C. D. Batista: J. Phys. Soc. Jpn. **85** (2016) 103703.

[9] R. Ozawa, S. Hayami, and Y. Motome: Phys. Rev. Lett. **118** (2017) 147205.

[10] 東京大学大学院工学系研究科 プレスリリース (2017.04.05 付)

[11] S. Hayami, R. Ozawa, and Y. Motome: preprint (arXiv:1703.07690).

[12] S. Hayami, R. Ozawa, and Y. Motome: Phys. Rev. B **94** (2016) 024424.

[13] S. Okumura, Y. Kato, and Y. Motome: preprint (arXiv:1704.01708).

[14] Y. Sugita and Y. Motome: J. Phys. Soc. Jpn. **85** (2016) 073709.

[15] S. Hayami, H. Kusunose, and Y. Motome: J. Phys. Soc. Jpn. **85** (2016) 053705.

[16] S. Hayami, H. Kusunose, and Y. Motome, J. Phys.: Cond. Matter **28** (2016) 395601.

[17] Y. Kato, K. Kimura, A. Miyake, M. Tokunaga, A. Matsuo, K. Kindo, M. Akaki, M. Hagiwara, M. Sera, T. Kimura, and Y. Motome: Phys. Rev. Lett. **118** (2017) 107601.

[18] Y. Sugita, T. Miyake, and Y. Motome: preprint (arXiv:1704.00318).

Thermal pure quantum state study on finite-temperature properties of quantum spin liquids

Takahiro Misawa
Institute for Solid State Physics, University of Tokyo
Kashiwa-no-ha, Kashiwa, Chiba 277-8581

The two-dimensional Hubbard model with geometrical frustrations is one of the simplest theoretical models that describes competition and cooperation of the strong electronic correlations and the geometrical frustrations. In this model, due to the next-nearest neighbor hopping t', which induces the next-nearest neighbor antiferromagnetic interactions, the competition between two magnetic phases occurs: Simple Néel state becomes stable when t' is small compared to the nearest neighbor hopping t while stripe state becomes stable for large t' region ($t'/t \sim 1$). Several theoretical calculations for the ground states of the frustrated Hubbard model including its strong coupling limit, i.e., frustrated J_1-J_2 Heisenberg, have been done so far. Most of previous calculations suggest that quantum spin liquid states actually appear [1, 2, 3, 4, 5] around intermediate region ($t'/t \sim 0.75$ or $J_2/J_1 \sim 0.5$). In spite of the huge amount of the studies for the ground states, there are few unbiased theoretical studies on the finite-temperature properties of the frustrated Hubbard model due to the lack of the efficient theoretical method.

Recently, efficient numerically unbiased method for calculating finite temperature properties in quantum systems is proposed [6]. In this method, it is shown that the calculation within small number of pure states instead of the full ensemble average is sufficient for accurate estimate of finite-temperature properties. Such pure states are called thermal pure quantum (TPQ) states and they are easily generated by performing the imaginary-time evolution of the wave function.

By using the TPQ method, we systematically study finite-temperature properties of the frustrated Hubbard model. As a result, around $t'/t \sim 0.75$, we find the evidence of the spin liquid states from the calculations on temperature dependence of the spin correlations and entropy. The present unbiased and detailed numerical calculations also offer an experimental criterion of closeness to the spin liquid phase: Finite-temperature entropy at moderate temperatures $T/t \sim 0.1$ significantly correlates with closeness to the spin liquid phase. We also find that such signatures of quantum spin liquid states can be observed in an ab initio models [7] for spin-liquid candidates $EtMe_3Sb[Pd(dmit)_2]_2$.

A part of calculation is done by using open-source software $\mathcal{H}\Phi$ [8].

References

[1] T. Kashima and M. Imada, J. Phys. Soc. Jpn. **70**, 3052 (2001).

[2] T. Mizusaki and M. Imada, Phys. Rev. B **74**, 014421 (2006).

[3] L. F. Tocchio, F. Becca, A. Parola, and S. Sorella, Phys. Rev. B **78**, 041101 (2008).

[4] H.-C. Jiang, H. Yao, and L. Balents, Phys. Rev. B **86**, 024424 (2012).

[5] W.-J. Hu, F. Becca, A. Parola, and S. Sorella, Phys. Rev. B **88**, 060402 (2013).

[6] S. Sugiura and A. Shimizu, Phys. Rev. Lett. **108**, 240401 (2012).

[7] K. Nakamura, Y. Yoshimoto, and M. Imada, Phys. Rev. B **86**, 205117 (2012).

[8] https://github.com/QLMS/HPhi.

Topological phases and nonequilibrium phenomena in strongly correlated electron systems with strong spin-orbit interaction

Norio KAWAKAMI
Department of Physics, Kyoto University
Kitashirakawa, Sakyo-ku, Kyoto 606-8502

Many quantum phases compete in systems with coexisting spin-orbit interaction and electron correlation. Particularly, topologically nontrivial band structures, which are classified by topological invariants, have attracted much attention experimentally and theoretically.

We have studied the impact of strong correlations on the surface states of a three-dimensional topological Kondo insulator. [1] Correlations are strongly increased at the surface and at low enough temperature T, the surface f electrons are energetically confined into a narrow window around the Fermi energy. While light and heavy surface states coexist, with increasing temperature, the latter becomes incoherent.

We have studied the modification of the competition between the Kondo effect and the RKKY interaction in f-electron materials by the superlattice structure. [2] The quantum critical point between the magnetic phase and the Fermi-liquid phase depends on the structure of the f-electron superlattice.

By analysing a bilayer Kane-Mele-Hubbard model with lattice distortion and interlayer spin exchange interaction under cylinder geometry using real-space dynamical mean field theory (R-DMFT) with continuous-time quantum Monte Carlo (CTQMC), we have demonstrated that a topological Mott insulating (TMI) state emerges. [3] The TMI state, which hosts gapless edge modes only in collective spin excitations, evolves from the ordinary spin-Hall insulating state with increasing the Hubbard interaction before it undergoes a phase transition to a trivial Mott insulator.

We have studied the reduction of topological classification in free fermions. In a bilayer honeycomb lattice model by taking into account temperature effects using R-DMFT+CTQMC, we have shown that even when the reduction occurs, the winding number ν defined by the Green's function can take a nontrivial value at $T = 0$, which is consistent with the absence of gapless edge modes due to edge Mott behaviors. [4] Furthermore, we have proposed a heavy fermion superlattice system as a test bed for the reduction of topological classification in free fermions. [5]

References

[1] R. Peters, T. Yoshida, H. Sakakibara, and N. Kawakami: Phys. Rev. B **93**, 235159 (2016).

[2] R. Peters, Y. Tada, and N. Kawakami: Phys. Rev. B **94**, 205142 (2016).

[3] T. Yoshida and N. Kawakami: Phys. Rev. B **94**, 085149 (2016).

[4] T. Yoshida and N. Kawakami: Phys. Rev. B **95**, 045127 (2017).

[5] T. Yoshida, A. Daido, Y. Yanase, and N. Kawakami: Phys. Rev. Lett. **118**, 147001 (2017).

Novel phenomena of correlated topological phases

Tsuneya Yoshida

Department of Physics, Kyoto University,

Sakyo-ku, Kyoto 606-8502

In this decade, topological insulators/superconductors have attracted much attention due to their interesting phenomena arising from topology of the ground state wave functions. So far, electron correlations have been neglected in most of studies of topological phases. Recently, however, it became clear that topological insulators can emerge even in strongly correlated systems. Furthermore such systems are expected to show new phenomena arising from electron correlation and topology. Therefore, understanding impact of electron correlation on topological insulators is one of the most important issues of condensed matter systems.

In our study, we have addressed this issue by making used of dynamical mean field theory (DMFT)[1-4] as well as bosonization approach[5]. Here, in particular, we focus topological phases in heavy-fermion systems.

(i) $CeCoIn_5$/$YbCoIn_5$ superlattice systems as a test bed for reduction of topological classification. Classifying of topological phases, i.e., examining how many topological phases exist under given symmetry, has provided useful information for searching topological materials. In 2010, Fidkowski and Kitaev revealed that the classification result may change in the presence of electron correlations; for instance, topological superconductors of symmetry class BDI can show topological phases characterized by an arbitrary integer, while there are only eight distinct topological phases in the presence of electron correlations. Namely, in this case, electron correlations reduce number of possible topological phases. The aforementioned reduction of topological classification is new phenomenon. Unfortunately, however, no candidate material has been reported so far. In our study, we have searched a candidate material which can show the reduction of topological classification. As the result, we have found the $CeCoIn_5$/$YbCoIn_5$ superlattice system can be the candidate material for the reduction of topological classifications $Z \times Z \rightarrow Z \times Z_8$[5]. Furthermore, we have analyzed finite temperature effects in a bi-layer honeycomb lattice model showing the reduction $Z \rightarrow Z_4$ by using DMFT+ continuous-time quantum Monte Carlo[2].

(ii) Temperature effects on topological Kondo insulators. Although the topological structure is well-defined only at zero

temperature, understanding finite temperature effects on topological insulators is important form a practical view point; any experiment is carried out at finite temperatures. Besides that, in heavy fermion systems, various intriguing behaviors have been reported for finite temperature regions due to the Kondo effect.

In our study, applying DMFT + numerical renormalization group method to the Kane-Mele Kondo lattice model[4], we have demonstrated that finite temperature effects can restore gapless edge modes even when gapless edge modes are destroyed at zero temperature. Furthermore, combining first principle calculation and the dynamical mean-field theory, we have revealed that the effective mass at the edge becomes much heavier than that in the bulk for SmB6, which may explain inconsistency of the mass between ARPES measurement and transport measurement[3].

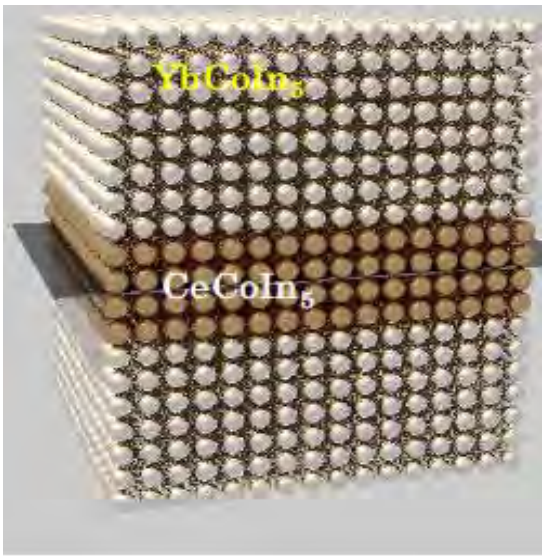

Fig. 1: Sketch of $CeCoIn_5/YbCoIn_5$ superlattice.

References

[1] Tsuneya Yoshida and Norio Kawakami: Phys. Rev. B **95** (2017) 045127.

[2] Tsuneya Yoshida and Norio Kawakami: Phys. Rev. B **94** (2016) 085149.

[3] Robert Peters, Tsuneya Yoshida, Hirofumi Sakakibara, and Norio Kawakami: Phys. Rev. B **93** (2016) 235159.

[4] Tsuneya Yoshida, Robert Peters and Norio Kawakami: Phys. Rev. B **93** (2016) 045138.

[5] Tsuneya Yoshida, Akito Daido, Youich Yanase, and Norio Kawakami: Phys. Rev. Lett. **118** (2017) 147001.

Competitions of superconducting, antiferromagnetic and charge orders in electron-phonon coupled systems

Takahiro OHGOE

Department of Applied Physics, The University of Tokyo,

7-3-1 Hongo, Bunkyo-ku, Tokyo 113-0033

In a class of strongly-correlated materials, the interplay between electron correlations and electron-phonon interactions is believed to induce novel phenomena such as the unconventional high-Tc s-wave SC in the alkali-doped fullerenes [1]. To establish the roles of phonons in a wide range of stongly correlated materials, we need a flexible method which can accurately treat strong electron-electron and electron-phonon interactions on an equal footing. In previous study, we proposed an extended many-variable variational Monte Carlo method [2] for electron-phonon coupled systems [3].

In this work, by using the many-variable variational Monte Carlo method, we study competitions of strong electron-electron and electron-phonon interactions in the ground state of Holstein-Hubbard model on a square lattice [4]. At half filling, an extended intermediate metallic or weakly superconducting (SC) phase emerges, sandwiched by antiferromagnetic (AF) and charge order (CO) insulating phases (Fig. 1). By the carrier doping into the CO insulator, the SC order dramatically increases for strong electron-phonon couplings, but largely hampered by wide phase separation (PS) regions. Superconductivity is optimized at the border to the PS.

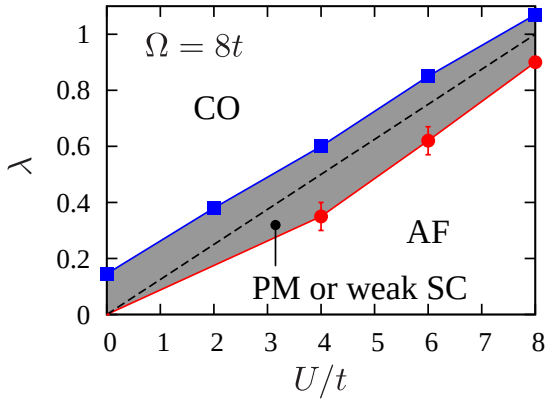

Fig. 1: Ground-state phase diagram of the Holstein-Hubbard model on a square lattice in the U/t-λ plane. Here, U/t is the on-site Coulomb interaction divided by the hopping amplitude, and λ is the dimensionless electron phonon interaction.

References

[1] Y. Nomura, S. Sakai, M. Capone, and R. Arita, Sci. Adv. 1, e1500568 (2015)

[2] D. Tahara and M. Imada, J. Phys. Soc. Jpn. **77**, 1140701 (2008)

[3] T. Ohgoe and M. Imada, Phys. Rev. B **89**, 195139(2014)

[4] T. Ohgoe and M. Imada, arXiv:1703.0889

DMFT study for the valence skipping and charge Kondo effect induced by pair hopping interaction

Akihisa Koga
Department of Physics, Tokyo Institute of Technology
Ookayama, Meguro, Tokyo 152-8551

Valence skipping has been observed in some compounds containing the group III, IV, V or VI element such as Bi or Tl. In these valence skipping elements, the ionic states with closed shell are stable rather than non-closed shell states. Recently, it has been reported that Tl-doped PbTe exhibits Kondo-like behavior in the resistivity in spite of the absence of magnetic impurities [1]. Moreover, superconductivity is also observed in this material at low temperatures [1, 2, 3], implying that the the valence skipping nature and charge Kondo effect [4] play a key role for the emergence of the superconductivity.

In previous theoretical works, the valence skipping nature has been explained by an effective negative Coulomb interaction [5]. On the other hand, recently, the valence skipping and charge Kondo effect have successfully been described, by introducing the impurity Anderson model with the pair hopping interaction, instead of the negative Coulomb interactions [6]. This indicates the importance of the pair hopping term for understanding the valence skipping behaviors and charge Kondo effect. However, it remains unclear how the pair hopping interaction affects physical properties in the lattice systems beyond the impurity model.

To investigate the valence skipping phenomenon and charge Kondo effect induced by pair hopping interaction in lattice systems, we analyze the extended Falicov-Kimball model on the Bethe lattice as follows:

$$\begin{aligned}\mathcal{H} = & -t \sum_{\langle i,j\rangle,\sigma} c^{\dagger}_{i\sigma} c_{j\sigma} + \epsilon_d \sum_{i,\sigma} n^d_{i,\sigma} \\ & + U_{cd} \sum_{i,\sigma,\sigma'} n^c_{i\sigma} n^d_{i\sigma'} \\ & - J_{ph} \sum_i (d^{\dagger}_{i\uparrow} d^{\dagger}_{i\downarrow} c_{i\uparrow} c_{i\downarrow} + \text{H.c.}), \end{aligned} \quad (1)$$

where $c_{i\sigma}$ ($d_{i\sigma}$) is the annihilation operator of a conduction (localized) electron with spin $\sigma(=\uparrow,\downarrow)$, respectively. $n^c_{i\sigma}(= c^{\dagger}_{i\sigma} c_{i\sigma})$ and $n^d_{i\sigma}(= d^{\dagger}_{i\sigma} d_{i\sigma})$ are the number operators of a conduction electron and an electron occupying the localized orbital at site i. t is the hopping integral of the conduction electrons between the nearest-neighbor sites, and U_{cd} and J_{ph} are the interorbital Coulomb interaction and pair hopping interaction, respectively. We assume that the localized orbital d corresponds to the electronic orbital of valence skipping elements.

In the work, we have used dynamical mean-field theory (DMFT) to clarify the stability of the charge Kondo effect in the lattice system. Here, we have made use of the continuous-time quantum Monte Carlo (CT-QMC) method with the double expansion technique as an impurity solver [7]. In this technique, we numerically perform the diagrammatic expansion for both hybridization between the impurity and bath, and the pair hopping term on an equal footing. This enables us to avoid the negative sign problem in the CT-QMC simulations. Moreover, we used the ALPS library preinstalled in the ISSP su-

percomputer system, which facilitates a parallelization in the present calculations [8].

We calculate the electron occupancy at each orbital and pseudo-spin correlations between the conduction and impurity orbitals introduced in Ref. [6]. We have found the charge ordered and s-wave superconducting phases. Performing the systematic calculations, we have clarified that the former (latter) is stabilized by the interaction U_{cd} (J_{ph}). In addition, we have found that the charge Kondo state appears in the strong pair hopping region.

References

[1] Y. Matsushita, H. Bluhm, T. H. Geballe, and I. R. Fisher, Phys. Rev. Lett. **94**, 157002 (2005).

[2] Y. Matsushita, P. A. Wianecki, A. T. Sommer, T. H. Geballe, and I. R. Fisher, Phys. Rev. B **74**, 134512 (2006).

[3] K. Nakayama, T. Sato, T. Takahashi, and H. Murakami, Phys. Rev. Lett. **100**, 227004 (2008).

[4] A. Taraphder and P. Coleman, Phys. Rev. Lett. **66**, 2814 (1991).

[5] T. Yanagisawa, I. Hase, Physica C **24-26**, 494 (2013)

[6] H. Matsuura and K. Miyake, J. Phys. Soc. Jpn. **81**, 113705 (2012).

[7] P. Werner, A. Comanac, L. de'Medici, M. Troyer and A. J. Millis, Phys. Rev. Lett. **97**, 076405 (2006)

[8] B. Bauer *et al.*, J. Stat. Mech. **2011**, P05001 (2011).

Numerical Studies on Excitation Spectra of Strongly Correlated Topological Materials

Youhei YAMAJI
Quantum-Phase Electronics Center and Department of Applied Physics, The University of Tokyo
Hongo, Bunkyo-ku, Tokyo 113-8656

The Kitaev's quantum spin liquid has attracted much attention as a rare example of controlled spin liquid ground state in correlated electron systems. An experimentally observable signature of proximity to the Kitaev's quantum spin liquid phase is a continuum in spin excitation spectra [1]. To examine the spin excitation spectra in the vicinity of the Kitaev's spin liquid phases, we employ the shifted Krylov subspace methods [2] and simulate dynamical spin structure factors of an *ab initio* effective hamiltonian of Na_2IrO_3 [3] and other related hamiltonians [4].

Below, we briefly touch on the shifted Krylov subspace method. Excitation spectra are given by taking imaginary parts of Green's functions defined as,

$$G^{AB}(\zeta) = \langle 0|\hat{A}^\dagger(\zeta - \hat{H})^{-1}\hat{B}|0\rangle. \tag{1}$$

To evaluate the above formula, the Lanczos method is widely employed. However, convergence of the Lanczos method often suffers from truncation errors. We have another option: We solve a linear equation by employing a conjugate gradient (CG) method, instead of explicitly calculating the resolvent of $\hat{H}$. The CG methods find the solution in a Krylov subspace, as follows. First, by introducing the following three vectors,

$$|\lambda\rangle = \hat{A}|0\rangle, \tag{2}$$
$$|\rho\rangle = \hat{B}|0\rangle, \tag{3}$$
$$|\chi(\zeta)\rangle = (\zeta - \hat{H})^{-1}|\rho\rangle, \tag{4}$$

we rewrite $G^{AB}(\zeta)$ as

$$G^{AB}(\zeta) = \langle\lambda|\chi(\zeta)\rangle. \tag{5}$$

To obtain the unknown vector $|\chi(\zeta)\rangle$, we solve the following linear equation,

$$(\zeta - \hat{H})|\chi(\zeta)\rangle = |\rho\rangle. \tag{6}$$

When the linear dimension of the matrix $\hat{H}$, $N_{\rm H}$, is too large to store the whole matrix in the memory, the linear equation is solved iteratively, for example, by using the CG methods. At nth iteration, the conjugate gradient algorithm initialized with $|\chi_0(\zeta)\rangle = |\rho\rangle$ finds an approximate solution $|\chi_n(\zeta)\rangle$ within a n-dimensional Krylov subspace $\mathcal{K}_n(\zeta - \hat{H}, |\rho\rangle) = \mathrm{span}\{|\rho\rangle, (\zeta - \hat{H})|\rho\rangle, \ldots, (\zeta - \hat{H})^{n-1}|\rho\rangle\}$. At each steps, the CG-type algorithms search the approximate solution $|\chi_n(\zeta)\rangle$ to minimize the 2-norm of the residual vector,

$$|\rho_n(\zeta)\rangle = (\zeta - \hat{H})|\chi_n(\zeta)\rangle - |\rho\rangle. \tag{7}$$

We note that one needs to solve Eq.(6) essentially once at a fixed complex number $\zeta = \omega + i\delta$ to obtain whole spectrum $-\mathrm{Im}G^{AB}(\omega + i\delta)$. Due to the shift invariance of the Krylov subspace [2], namely, $\mathcal{K}_n(\zeta - \hat{H}, |\phi\rangle) = \mathcal{K}_n(\zeta' - \hat{H}, |\phi\rangle)$ for any complex number $\zeta' \neq \zeta$, we can obtain $|\chi(\zeta')\rangle$ from $|\chi(\zeta)\rangle$ without performing time-consuming matrix-vector products [2]. The Krylov subspace methods utilizing the shift invariance are called the shifted Krylov subspace methods. The several shifted Krylov subspace methods are available through a numerical library $\mathcal{K}\omega$ [5].

As a typical example of the excitation spectra in the proximity to the Kitaev's spin liquid phase, we show dynamical spin structure factors of the *ab initio* effective hamiltonian of Na_2IrO_3 [3] in Fig.1. The contiuum spectra up to the typical energy scale of Na_2IrO_3, 30 meV, is a signature of the proximity. We also apply the shifted Krylov subspace method to simulating excitation spectra of the Kitaev-Γ model [4], which is relevenat to another Kitaev material α-$RuCl_3$.

To further examine the relevance of the the *ab initio* effective hamiltonian to Na_2IrO_3, the ground state properties of the *ab initio* effective hamiltonian are examined by combining tensor network approaches and exact diagonalization [6]. The proximity to the quantum spin liquids, other than the Kitaev's one, is also clarified in the t-t' Hubbard model [7]. These simulations have offered not only deeper understanding of the proximity to the spin liquid, but also benchmark results on newly implemented functions of $\mathcal{H}\Phi$ [8, 9].

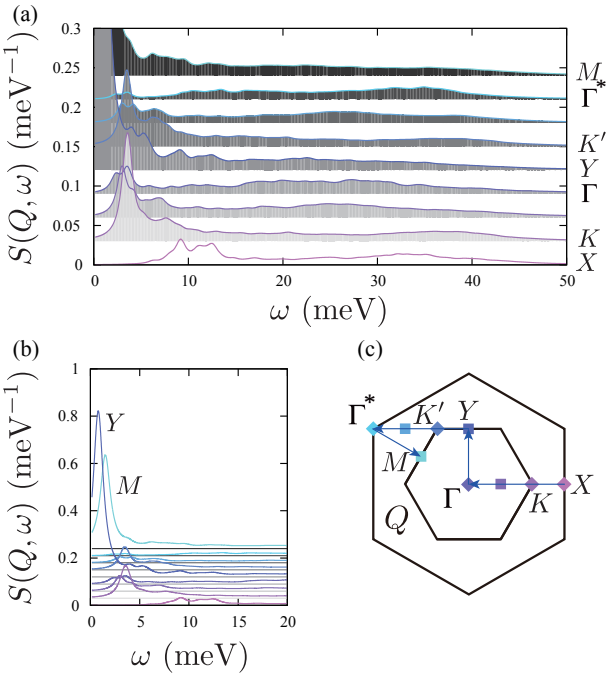

Figure 1: (a) Dynamical spin structure $S(Q,\omega)$ factors shifted vertically depending on Q. (b) Expansion of low-energy spectra. There are prominent peaks at the momenta Y and M, which correspond to zigzag orders observed in experiments. (c) Brillouin zone of Na_2IrO_3. Here, Γ^* corresponds to the standard Néel order.

References

[1] A. Kitaev, Annals Phys. **321** (2006) 2 (2006); J. Knolle, D. L. Kovrizhin, J. T. Chalker, and R. Moessner, Phys. Rev. Lett. **112** (2014) 207203.

[2] A. Frommer, Computing **70** (2003) 87.

[3] Y. Yamaji, T. Suzuki, T. Yamada, S. Suga, N. Kawashima, and M. Imada: Phys. Rev. B **93** (2016) 174425.

[4] A. Catuneanu, Y. Yamaji, G. Wachtel, H.-Y. Kee, and Y. B. Kim: arXiv:1701.07837.

[5] `https://github.com/issp-center-dev/Komega`

[6] T. Okubo, K. Shinjo, Y. Yamaji, N. Kawashima, S. Shigetoshi, T. Tohyama, and M. Imada: arXiv:1611.03614.

[7] T. Misawa and Y. Yamaji: arXiv:1608.09006.

[8] M. Kawamura, K. Yoshimi, T. Misawa, Y. Yamaji, S. Todo, and N. Kawashima: arXiv:1703.03637; accepted by Comput. Phys. Commun.

[9] `https://github.com/QLMS/Hphi/releases`

Monte Carlo approach to correlated electron and spin systems

Shintaro HOSHINO
RIKEN Center for Emergent Matter Science (CEMS), Wako 351-0198, Saitama, Japan

The discovery of a new type of ordered state of condensed matter is certainly an important and rare event. It is even nicer if the properties of this unconventional ordered state convincingly explain recent puzzling experimental results on an interesting class of correlated electron materials. In our recent work for correlated electrons using the supercomputer at Institute for Solid State Physics (ISSP), we show that certain types of three-orbital lattice systems, with degenerate orbital degrees of freedom, can spontaneously break the orbital symmetry in such a way that the electrons in a subset of orbitals are Mott insulating, while the electrons in the remaining orbitals are metallic (spontaneous orbital selective Mott transition). This state occurs in systems with effectively negative Hund coupling, such as fulleride compounds, and it can explain the origin of the puzzling "Jahn-Teller metal phase" that has been experimentally detected in $Rb_xCs_{3-x}C_{60}$ [1].

Alkali doped fulleride compounds [2, 3, 4] have attracted much attention due to their unconventional high Tc (∼38K) superconductivity. It is important to understand the properties of these correlated systems in the vicinity of the Mott phase, and to clarify the connection of the unconventional metal states to the superconducting instability. It has been suggested that the Jahn-Teller metal [1], which appears between the Mott insulating and unconventional superconducting phase of A_3C_{60}, may be characterized by the coexistence of itinerant and localized electrons.

To understand this peculiar behavior, we have analyzed the multiorbital Hubbard model with antiferromagnetic Hund coupling relevant to fulleride superconductors. For theoretical analysis, we have used the dynamical mean-field theory combined with the continuous-time quantum Monte Carlo method (hybridization expansion algorithm) [5]. This is suitable for strongly correlated three-dimensional electron systems such as fulleride compounds. The quantum Monte Carlo simulation has been performed efficiently by a parallel computing using the supercomputer facilities of ISSP.

Analyzing the multiorbital Hubbard model, we have numerically mapped out the phase diagrams which are shown in Fig. 1 together with the sketches for expermental phase diagrams [6]. Our results have succeeded to capture the characteristic phases observed in fulleride superconductors, including Jahn-Teller metal phase which is here identified as a spontaneous orbital selective Mott (SOSM) state. This ordered state is not characterized by any conventional one-body order parameter (it has no ordinary orbital moment, with broken orbital symmetry), but by a many-body operator. It is a so-called composite order, and it can also be viewed as an odd-frequency order because the symmetry-breaking appears in the time-dependence of certain correlation functions. The spontaneous orbital-selective Mott state is therefore a diagonal-order version of the concept of odd-frequency superconductivity.

References

[1] R.H. Zadik et al., Sci. Adv. **1**, e1500059 (2015).

[2] A.F. Hebard et al., Nature **350**, 600 (1991).

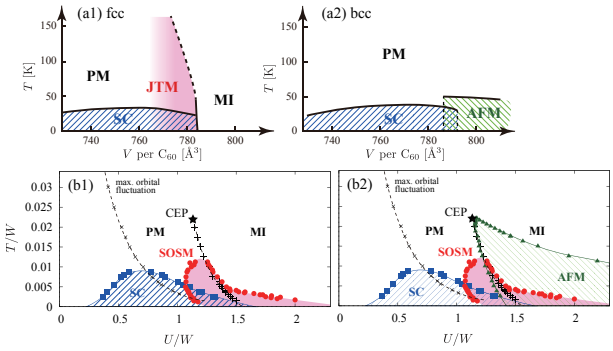

Figure 1: Sketches of the experimental phase diagrams for (a1) fcc and (a2) bcc fullerides based on Refs. [3, 1]. Panels (b1) and (b2) show the phase diagrams of the three-orbital Hubbard model for negative Hund coupling, without and with staggered orders, respectively. The former phase diagram corresponds to the fcc lattice since the geometrical frustration suppresses the staggered orders in a wide temperature range. See Ref. [6] for more detail.

[3] Y. Takabayashi et al., Science **323**, 1585 (2009).

[4] M. Mitrano et al., Nature **530**, 461 (2016).

[5] E. Gull et al., Rev. Mod. Phys. **83**, 349 (2011).

[6] S. Hoshino and P. Werner, arXiv:1609.00136, accepted for publication in Phys. Rev. Lett.

Numerical Studies on Models of Unconventional Superconductors

KAZUHIKO KUROKI
Department of Physics, Osaka University
1-1 Machikaneyama, Toyonaka, Osaka, 560-0043, Japan

In this report, we present two of the studies, related to superconductivity due to electron correlation, performed in our group in 2016 fiscal year using the supercomputer at ISSP.

SUPERCONDUCTIVITY IN SYSTEMS WITH ELECTRON AND HOLE BANDS

In the early days of the theoretical studies of the iron-based superconductors, the nesting of the Fermi surface was considered to be the key for the superconductivity. However, later experiments have suggested that high T_c is obtained when the nesting is degraded, or even in the absence of the nesting. In a previous study, we have pointed out that superconductivity is enhanced, even if the nesting is not good, if the magnitude of the hopping integrals is in good match with the inverse Fourier transformation of the gap function from momentum space to real space[1]. The importance of the real space picture implies that the states away from the Fermi level also plays an important role, since the inverse Fourier transformation from momentum space to real space involves all the states within the Brillouin zone, namely, the states away from the Fermi level.

Extending the above picture, we have studied how the finite energy spin fluctuation can act as a pairing glue. We apply the fluctuation exchange approximation to Hubbard type models possessing electron and hole bands, and compared them with the Hubbard model on a square lattice with a large Fermi surface[2]. As models with the electron and hole bands, we consider the five orbital model for the hydrogen doped 1111 iron-based superconductor, constructed in ref.1, and also a bilayer model with bonding and antibonding bands. In these models with electron and hole bands, superconductivity is optimized when the Fermi surface nesting is degraded to some extent, and finite energy spin fluctuations around the nesting vector develops. This is in contrast to the case of the square lattice model, where superconductivity is more enhanced for better nesting. The difference lies in the robustness of the nesting vector, namely, in models with electron and hole bands, the wave vector at which the spin susceptibility is maximized is fixed even when the nesting is degraded, whereas when the Fermi surface is large, the nesting vector varies with the deformation of the Fermi surface.

ELECTRON-HOLE ASYMMETRY OF THE ELECTRON CORRELATION STRENGTH IN THE CUPRATE SUPERCONDUCTORS

Recent experiments have revealed a remarkable difference in the phase diagram of the cuprate superconductors between hole- and electron-doped materials. Previously, there has been an understanding that pseudogap exists in both hole-doped and electron-doped cuprates. However, recent experiment shows that the pseudogap disappears in the electron-doped cases if the antiferromagnetism is suppressed by appropriate annealing process[3]. Hence, in the absence of the antiferromagnetism, there is an electron-hole asymmetry regarding the presence/absence of the pseudogap. Since the pseudogap can be considered as a hallmark of strong correlation, it seems that the strength of the electron correlation is apparently different between the electron and the hole-doped cases. One may consider that the origin of this asymmetry lies in the difference in the effective electron-electron interaction strength between the hole- and electron-doped materials. However, a recent first principles estimation[4] has revealed that many of the hole-doped cuprates have on-site U comparable to those in the T-type electron doped systems. A typical example with a moderate U is $HgBa_2CuO_4$, in which T_c is very high ($\sim$ 100K) and a pseudogap is observed. Therefore, it is difficult to explain the electron-hole asymmetry in the diagram by their interaction strength.

Given this background, we have analyzed the one-particle spectrum of the single band model of a cuprate superconductor using dynamical mean field theory with two kinds of impurity solvers : iterated perturbation theory and continuous time quantum Monte Carlo methods[5]. We have found that the electron-hole asymmetry of the electron correlation effect can exist even under common interaction strengths and the band structure between the hole- and electron-doped systems. Although there exists an asymmetric feature of the density of states, this alone cannot account for the remarkable asymmetry observed experimentally. An important finding is that the presence of the strong correlation effect, strong enough to produce a Mott insulating state

at half-filling, is necessary to understand the experimental observation. To be more precise, the combination of the Mottness and the asymmetry of the DOS results in a discontinuous electron-hole asymmetry of the one-particle spectrum. The fact that the present results are obtained under a common value of U between the hole and the electron-doped cases implies that the electron correlation effect is less visible in the electron-doped regime. In this sense, it can be said that the origin of the electron-hole asymmetry of the cuprates is the asymmetry of the "visibility" of the strong correlation effect.

[1] K. Suzuki, H. Usui, S. Iimura, Y. Sato, S. Matsuishi, H. Hosono, and. K. Kuroki, Phys. Rev. Lett. **113**, 027002 (2014).
[2] M. Nakata, D. Ogura, H. Usui and K. Kuroki, submitted.
[3] M. Horio *et al.*, Nat. Commmun. **7**, 10567 (2016).
[4] S. Jang, H. Sakakibara, H. Kino, T. Kino, K. Kuroki, and M.J.Han, Sci. Rep. **6**, 33397 (2016).
[5] R. Mizuno, M. Ochi, and K. Kuroki, submitted.

Research on Kondo effect in the Peierls-Anderson model

Dai MATSUI and Takashi HOTTA
Department of Physics, Tokyo Metropolitan University
1-1 Minami-Osawa, Hachioji, Tokyo 192-0397

After the discovery of magnetically robust heavy-fermion phenomenon in Sm-based filled skutterudites [1], non-magnetic Kondo effect due to electron-phonon interaction has attracted renewed attention in the research field of condensed matter physics. To promote our understanding on electronic properties of cage-structure compounds, it has been considered that *rattling*, i.e., local anharmonic oscillation of guest atom in the cage, plays a key role through the coupling with conduction electrons. Such rattling-induced phenomena have been frequently discussed on the basis of the Holstein-type model with the linear coupling between electron density and atomic displacement [2], given by $H_{\rm H} = g\rho x$, where g indicates an electron-phonon coupling, ρ is local electron density, and x denotes the displacement of atom. On the other hand, since localized electrons exist on the vibrating atom in the cage and conduction electrons originate from the atoms forming the cage, it is important to consider Peierls-type phonon in the hybridization between localized and conduction electrons, given by $H_{\rm P} = g\sum_{\boldsymbol{k},\sigma} x(d_\sigma^\dagger c_{\boldsymbol{k}\sigma} + {\rm h.c.})$, where $d_\sigma^\dagger$ and $c_{\boldsymbol{k}\sigma}$ denotes the annihilation operators of localized and conduction electrons, respectively, σ is spin, and $\boldsymbol{k}$ indicates wave vector.

In this research, we discuss the Kondo effect in the Peierls-Anderson model. The Hamiltonian is given by

$$H = \sum_{\boldsymbol{k}\sigma} \varepsilon_{\boldsymbol{k}} c_{\boldsymbol{k}\sigma}^\dagger c_{\boldsymbol{k}\sigma} + H_0, \tag{1}$$

where $\varepsilon_{\boldsymbol{k}}$ is the dispersion of conduction electron and H_0 includes the hybridization and local terms, given by

$$\begin{aligned} H_0 = {} & U n_\uparrow n_\downarrow + E_d \rho + \omega a^\dagger a \\ & + U_{\rm dc} \sum_{\boldsymbol{k},\boldsymbol{k}',\sigma} c_{\boldsymbol{k}\sigma}^\dagger c_{\boldsymbol{k}'\sigma} \rho \\ & + V_{\rm P} \sum_{\boldsymbol{k}\sigma} (a + a^\dagger)(d_\sigma^\dagger c_{\boldsymbol{k}\sigma} + {\rm h.c.}). \end{aligned} \tag{2}$$

Here U denotes the Coulomb interaction between localized electrons, $n_\sigma = d_\sigma^\dagger d_\sigma$, $\rho = n_\uparrow + n_\downarrow$, E_d is the energy level of localized electron, a is the annihilation operator of Peierls phonon, ω is the phonon energy, $U_{\rm dc}$ indicates the Coulomb interaction between localized and conduction electrons, and $V_{\rm P}$ denotes the phonon-assisted hybridization. Note that the energy unit is a half of the conduction bandwidth, which is set as unity in the following calculations. In this unit, we set $U = 1$ and $\omega = 0.1$. As for E_d, we set $E_d = -U/2$ to consider the case of half filling at an impurity site. Then, we change $V_{\rm P}$ and $U_{\rm dc}$ to investigate electronic and phononic properties. We also note that it is useful to define the non-dimensional coupling constant α through $V_{\rm P} = \sqrt{\alpha}\omega$. Roughly speaking, the cases of $\alpha < 1$ and $\alpha > 1$ correspond to the weak- and strong-coupling regions, respectively.

Here we note the conserved quantity in the Peierls-Anderson model, in addition to charge and spin. Namely, we define parity P as

$$P = \rho + N_{\rm ph} \bmod 2, \tag{3}$$

where $N_{\rm ph}$ indicates the phonon number. The states with $P = 0$ and 1 correspond to even and odd parity ones, respectively. We note that the eigenstates of H_0 are characterized by P in addition to total charge and spin. Note also that for $U_{\rm dc} = U/2$, it is possible to obtain the exact solution of H_0 (the two-site problem) by using Lang-Firsov transformation. We find that even and odd parity states are exactly degenerate for $U_{\rm dc} = U/2$.

To investigate the electronic and phononic properties of H at low temperatures, we usually discuss the corresponding susceptibilities, entropy, and specific heat. For the diagonalization of the impurity Anderson model, we employ a numerical renormalization group (NRG) method, in which we logarithmically discretize the momentum space so as to efficiently include the conduction electrons near the Fermi energy. The conduction electron states are characterized by "shells" labeled by N, and the shell of $N = 0$ correspond to the two-site case described by H_0. Then, after some algebraic calculations, the Hamiltonian is transformed into the recursive form

$$H_{N+1} = \sqrt{\Lambda} H_N + \xi_N \sum_\sigma (c^\dagger_{N\sigma} c_{N+1\sigma} + c^\dagger_{N+1\sigma} c_{N\sigma}), \quad (4)$$

where Λ is a parameter used for logarithmic discretization, $c_{N\sigma}$ denotes the annihilation operator of the conduction electron in the N-shell, and ξ_N indicates the "hopping" of the electron between N- and $(N+1)$-shells, expressed by

$$\xi_N = \frac{(1+\Lambda^{-1})(1-\Lambda^{-N-1})}{2\sqrt{(1-\Lambda^{-2N-1})(1-\Lambda^{-2N-3})}}. \quad (5)$$

In the NRG calculation, we keep M low-energy states for each renormalization step. In this study, we set $\Lambda = 5.0$ and $M = 2000$.

In the weak-coupling region, we obtain the standard spin Kondo effect for $U_{\rm dc} < 1$, while the singlet even-parity state appears for $U_{\rm dc} > 1$. On the other hand, in the strong-coupling region, we find the Schottky-type specific heat.

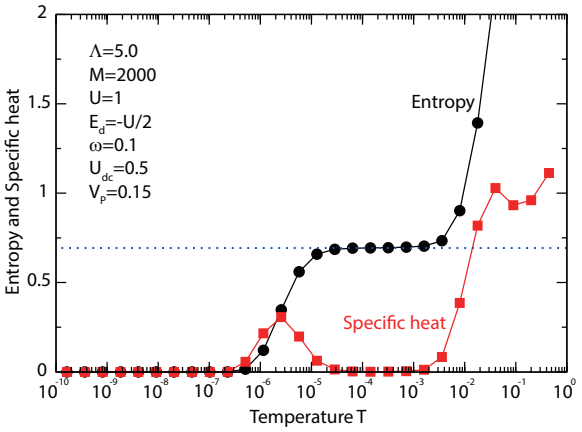

Figure 1: Entropy $S_{\rm imp}$ (solid circle) and specific heat $C_{\rm imp}$ (solid square) for $U = 1$, $E_d = -U/2$, $U_{\rm dc} = 0.5$, $V_{\rm P} = 0.15$, and $\omega = 0.1$. The dotted line indicates $\log 2$.

In Fig. 1, we show typical results for entropy and specific heat in the strong-coupling region for $U_{\rm dc} = U/2$. We observe the plateau of $\log 2$ and the release of this entropy leads to the peak in the specific heat. Note that this entropy release is due to the lift of parity doublet, not due to the Kondo effect. In fact, when we evaluate the energy difference Δ between even and odd parity states for 4-site case, it is found that the peak temperature is in proportion to Δ. This phenomenon is, of course, characterized by the change of parity susceptibility, but this is only a theoretical quantity. For the comparison with experimental results, we propose the measurement of the electric dipole susceptibility, which reproduces the temperature dependence of parity susceptibility in the strong-coupling region.

References

[1] S. Sanada, Y. Aoki, H. Aoki, A. Tsuchiya, D. Kikuchi, H. Sugawara, and H. Sato: J. Phys. Soc. Jpn. **74** (2005) 246.

[2] T. Hotta: J. Phys. Soc. Jpn. **78** (2009) 073707.

Magnetic properties in the Hubbard model on the Honeycomb Lattice by variational cluster approximation

Atsushi Yamada
Department of Physics, Chiba University
Chiba 263-8522, Japana, Chiba 277-8581

A spin liquid state, which is a purely non-magnetic Mott insulator without spontaneously broken spatial or spin symmetry, has attracted a lot of interest. This state is realized in geometrically frustrated systems like the charge organic transfer salts κ-(BEDT-TTF)$_2$X[1] and Cs_2CuCl_4.[2] A simple theoretical model of these compounds is the Hubbard model on the an-isotropic triangular lattice, and spin liquid state is in fact found in this model.[3] A spin liquid could arise also in the intermediate coupling region of strongly correlated systems between a semimetal and ordered state, because in this case a correlation-driven insulating gap might open before the system becomes ordered. This possibility might be realized in the half-filled Hubbard model on the honeycomb lattice.

We have studied the magnetic and metal-to-insulator transitions by variational cluster approximation using 10-site and 16-site clusters as a reference system. Parts of numerical calculations were done using the computer facilities of the ISSP. We found that $U_{\rm AF} = 2.7$ and $U_{\rm MI} = 3.0$ for 10-site cluster, and $U_{\rm AF} = 2.7$ and $U_{\rm MI} = 3.2$ for 16-site cluster.[5] This result also rules out the existence of the spin liquid in this model. Both the magnetic and non-magnetic metal-to-insulator transitions are of the second order. Our results agree with recent large scale Quantum Monte Carlo simulations.[4]

References

[1] Y. Shimizu, K. Miyagawa, K. Kanoda, M. Maesato, and G. Saito, Phys. Rev. Lett. **91**, 107001 (2003); Y. Kurosaki, Y. Shimizu, K. Miyagawa, K. Kanoda, and G. Saito, Phys. Rev. Lett. **95**, 177001 (2005).

[2] R. Coldea, D.A. Tennant, A.M. Tsvelik, and Z. Tylczynski, Phys. Rev. Lett. **86**, 1335 (2001); R. Coldea, D.A. Tennant, and Z. Tylczynski, Phys. Rev. Lett. **68**, 134424 (2003).

[3] T. Yoshioka, A. Koga, and N. Kawakami, Phys. Rev. Lett. **103**, 036401 (2009); P. Sahebsara and D. Sénéchal, Phys. Rev. Lett. **100**, 136402 (2008); L.F. Tocchio, H. Feldner, F. Becca, R. Valenti, and C. Gros, Phys. Rev. B **87**, 035143 (2013); A. Yamada, Phys. Rev. B **89**, 195108 (2014); L.F. Tocchio, C. Gros, R. Valentí, F. Becca, Phys. Rev. B **89**, 235107 (2014); A. Yamada, Phys. Rev. B **90**, 235138 (2014).

[4] S. Sorella, Y. Otsuka, and S. Yunoki, Sci. Rep. **2**, 992 (2012); F. F. Assaad and I. F. Herbut, Phys. Rev. X **3**, 031010 (2013); F. Parisen Toldin, M. Hohenadler, F. F. Assaad, and I. F. Herbut, Phys. Rev. B **91**, 165108 (2015).

[5] A. Yamada, Int. J. Mod. Phys. B **30**, 1650158 (2016).

Monte Carlo simulation of ^{4}He adsorbed on substrates[*]

Yuichi MOTOYAMA
Institute for Solid State Physics, University of Tokyo
Kashiwa-no-ha, Kashiwa, Chiba 277-8581

A system of ^{4}He atoms adsorbed on a substrate such as a graphite is an ideal two-dimensional interacting bosonic system. Greywall [1] studied ^{4}He on a graphite by measuring heat capacity and drew a phase diagram consisting of 1/3 solid phase, fluid and solid coexistence phase, normalfluid and superfluid coexistence phase, and normal fluid phase. This diagram is compatible with that of a hardcore Bose-Hubbard model with nearest neighbor repulsion on a triangular lattice in quality. On the other hand, Pierce and Manousakis [2] performed path integral quantum Monte Carlo (PIQMC) calculation of ^{4}He on a graphite and reported that solid-vacuum coexistence phase extended to very low density at very low temperature, and there is no superfluid phase.

Aiming to perform larger simulation, we tried to obtain an effective lattice Hamiltonian for ^{4}He atoms on a graphite surface, because PIQMC for continuous space has not been yet parallelized but PIQMC for lattice system is already massively parallelized [3]. We have at least three ways to obtain parameters of an effective Hamiltonian. The first one is starting from adsorption sites, that is, to use the tight-binding representation to build an effective model. In this representation, we compare worldlines of continuous space system with that of lattice system. Another method is to discretize continuous space. This is straightforward but obtained effective model including many interactions, say, n-th nearest neighbor coupling. The last strategy is brute force method, which is to search for parameters reproducing results, such as melting point, from continuous space Monte Carlo method.

In this study, we adopted the first strategy and tried to estimate a hopping constant t of an effective model as the following way. First, we performed continuous space Monte Carlo simulation and obtained imaginary-time trajectories (snapshots) of a ^{4}He atom. Second, we regarded a circle centered on an adsorption site with a fixed radius dr as a "site" of an effective model. Next, we counted the number of hopping from one "site" to another "site" and calculated mean time between hopping, $\langle \mathrm{d}t \rangle$. Finally, we estimated the hopping constant of an effective hardcore Bose-Hubbard model on a triangular lattice t as $t = 1/(6\langle \mathrm{d}t \rangle)$, where 6 is the coordination number of a triangular lattice. Figure 1 shows dr dependence of the estimated hopping constant of an effective model for ^{4}He on a graphite surface. If particles are tightly bounded to "site", t will saturate before a "site" completely covers a hexagon of carbons (d$r \sim 1.42$Å). ^{4}He on a graphite, however, is not the case, and so this system cannot be represented by the tight-binding model.

References

[*] This work has been done in collaboration with A. Masaki-Kato and N. Kawashima.

[1] D. S. Greywall, Phys. Rev. B **47**, 309 (1993).

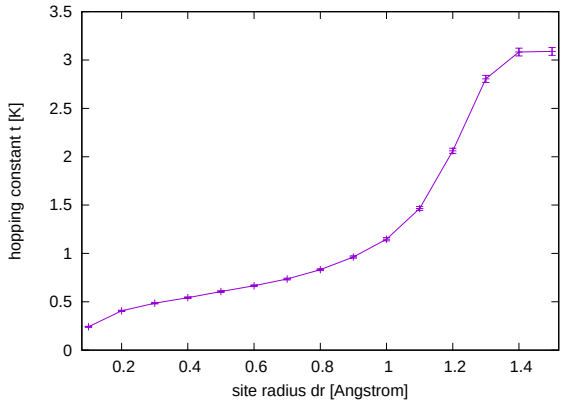

Figure 1: "site" radius dr dependence of the estimated hopping constant t of an effective lattice model for ^{4}He on a graphite surface.

[2] M. E. Pierce and E. Manousakis, Phys. Rev. B **62**, 5228 (2000).

[3] A. Masaki-Kato, T. Suzuki, K. Harada, S. Todo, and N. Kawashima, Phys. Rev. Lett **112**, 140603 (2014).

First-principles study on strong electron correlations in 5d transition metal oxides

Hiroshi Shinaoka
Department of Physics, Saitama University
Sakura-ku, Saitama-shi, Saitama, Japan, 338-8570

In recent years, novel properties of $5d^5$ pyrochlore iridates have been studied extensively theoretically and experimentally. We have studied metal-insulator and magnetic transitions in $Y_2Ir_2O_7$ by means of the local density approximation+dynamical mean-field method (DFT+DMFT). [2] For this study, we implemented a quantum Monte Carlo impurity solver based on the hybridization expansion algorithm [1], which can treat complex hybridization functions. This year, we have further implemented the measurement of various correlation functions such as two-particle Green's function in the solver. This new feature will be useful for investigating dynamical spin-orbital correlations in these compounds. The code has been published as an open-source software licensed under GPLv3. [3] The code is built on an updated version of the core libraries of ALPS (Applications and Libraries for Physics Simulations) [ALPSCore libraries].

We used the new impurity solver to investigate a $5d^4$ pyrochlore oxide, $Y_2Os_2O_7$. This compound is the first $5d^4$ pyrochlore oxide whose low-T properties have been reported experimentally. In the presence of strong spin-orbit coupling (SOC), the three t_{2g} orbitals are split into an upper $j_{\rm eff}$=1/2 doublet and a lower $j_{\rm eff} = 3/2$ quartet. If the SOC is strong enough, a d^4 configuration will be a trivial band insulator with four electrons filling the lower $j_{\rm eff} = 3/2$ manifold. Surprisingly, it has been reported that $Y_2Os_2O_7$ is an magnetically active insulator whose magnetic susceptibility follows a Curie-Weiss-like law below room temperature but does not show any magnetic long-range order down to 10 K. This may indicate the existence of a novel insulating phase induced by strong electron correlation and geometrical frustration.

We first figured out a U-$J_{\rm H}$ phase diagram (U is onsite Coulomb repulsion and $J_{\rm H}$ is Hund's coupling). In the DFT+DMFT calculations, we used a rotationally invariant Slater-Kanamori interaction. We constructed maximally localized Wannier functions for t_{2g} manifold. Most of the simulations were carried out on the system B.

We plot the spectral function at $\omega = 0$ computed with $\beta = 40$ eV ($T \simeq 290$ K) in Fig. 1. The spectral weight $A(\omega = 0)$ vanishes around $U = 2$ eV for reasonable values of $J_{\rm H}/U = 0.1$–0.2. For (possibly unphysical) large values of the Hund's coupling, the system enters into a metallic phase where the above mentioned single-particle picture is not valid due to strong hybridizations between the two manifolds.

Now we focus on the results obtained with $J_{\rm H}/U = 0.1$. We plot computed momentum-resolved spectral function $A(k, \omega)$ in Fig. 1. It is clearly seen that as U increases the system exhibits a Lifsitz transition to a band insulator where quasi-particle bands still survive. To investigate the magnetic properties more closely, we computed the correlation function $\langle \hat{M}(\tau)\hat{M}(0)\rangle$ in imaginary time, where $\hat{M}$ is a local magnetic moment operator (including spin and orbital contributions). We used

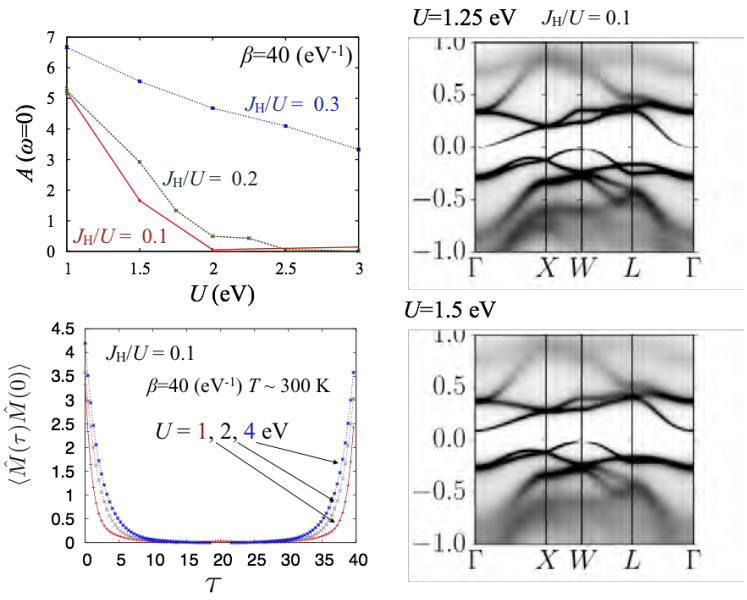

Figure 1: Spectral weight at $\omega = 0$, the momentum-resolved spectral weight $A(k, \omega)$, and the imaginary-time correlation function of magnetic moments.

the ability of the impurity solver to compute two-particle correlation functions. As shown in the figure, the correlation function quickly decays toward $\tau = \beta/2$, indicating that the ground state is magnetically inactive (.i.e., the ground state is a nonmagnetic band insulator). These results contradict the experimental results. This may indicate the important of non-local correlation functions beyond the DFT+DMFT approximation.

This work on $Y_2Os_2O_7$ was done in collaboration with Youhei Yamaji (University of Tokyo).

References

[1] P. Werner, A. Comanac, L. def Medici, M. Troyer, A. Millis, Phys. Rev. Lett. **97**, 076405 (2006).

[2] H. Shinaoka, S. Hoshino, M. Troyer, P. Werner, Phys. Rev. Lett. **115**, 156401(1-5) (2015).

[3] H. Shinaoka, E. Gull, P. Werner, Computer Physics Communications **215**, 128–136 (2017).

Topological symmetry in two-body scattering in strongly correlated electron systems

Koichi KUSAKABE
Graduate School of Engineering Science, Osaka University
1-3 Machikaneyama, Toyonaka, Osaka 560-8531

1. Introduction

Topological symmetry found in materials causes symmetry protected two-particle interaction processes. In curious materials, *e.g.* nanographene and cuprate superconductors, we often find a selected set of relevant orbitals, where the scattering processes among them are strongly optimized to cause "exchange-mediated correlation effects" and "the enhanced super processes". We can derive the scattering strength and specialty of the resulted electron state via the multi-reference density functional theory (MR-DFT).

2. The A-space formulation of MR-DFT

In our MR-DFT,[1, 2] we define a set A of orbitals for the correlated electron sub-system. This is usually done by obtaining the Kohn-Sham orbitals via a self-consistent calculation. A projection operator P_A giving a representation state $|\Psi_A\rangle \equiv P_A|\Psi\rangle = |\Phi_A\rangle \times |\Phi_0\rangle$ is defined for the MR ground state $|\Psi\rangle$, where $|\Phi_0\rangle$ is an uncorrelated filled state and $|\Phi_A\rangle$ is the strongly correlated state in the effective model. The representation state is determined via a many-body effective Hamiltonian in a form of

$$\left(\hat{H}_A + \hat{h}_B + \hat{H}_{\rm super}\right)|\Psi_A\rangle \quad = \quad E|\Psi_A\rangle. \quad (1)$$

Here, the third term in the Hamiltonian represents the super processes, which may describe screening, super exchange, pair hopping, and all of renormalized effective interactions.

$$\hat{H}_{\rm super} = P_A\hat{H}_{AB} \left(E - \hat{H}_A - \hat{h}_B - P_B\hat{H}_{AB} - \hat{H}_{BA}\right)^{-1} \hat{H}_{BA}P_A.$$

This Brillouin-Wigner-type determination equation is exact for a MR-DFT model where inter-particle interactions are subtracted in the un-correlated sub sets for both of the filled and empty orbitals in $|\Phi_0\rangle$.[3]

3. A spin-exchange process for Kondo's screening in nanographene

A set of topologically protected zero modes is found for a series of nanographene molecules called the vacancy-centered arm-chair-edged hexagonal nanographene (VANG).[4] These modes are producing a protected Kondo screening promoting formation of the stable singlet ground state with strong entanglement between a quasi-localized electron and Dirac electrons by the super process. This protection is caused by a topological protection of zero modes found in VANG.[5] When the molecule is deformed, if a mirror symmetry axis is preserved, the singlet formation via the exchange scattering is maintained.

The VANG molecules provides us a unique opportunity for fabrication of efficient hydrogen storage materials.[6, 7, 8] We have derived a special chemical reaction against hydrogen adsorption on VANG, where the barrier height is much reduced than conventional storage materials composed of organic hydrides.

We offered new fabrication and design methods of edges states at the armchair edges,[9] which is promising for controllable quantum device. This example is explained by the topological argument by Ryu-Hatsugai.

4. Materials dependence of cuprate superconductors

A self-doping effect between outer and inner CuO_2 planes (OPs and IPs) in multi-layer cuprate superconductors is investigated theoretically. When one considers a three-layer tight-binding model of the Hg-based three-layer cuprate derived from the single-reference DFT, the electron concentration tends to be large in the OP compared to the IP, which is opposite to the experimental fact. While the two-particle self-consistent approach for multi-layer systems by Nishiguchi[10] derives decrease in the double occupancy (instability for the antiferromagnetic phase) apparently in OP than IP in a three-layer Hubbard model, which corresponds to the strongly correlated phase of MR-DFT.

To explore material dependence of layered cuprate superconductors, we examine effective two-particle interactions for Hg1201 and Tl1201, where Tl1201 having a nearly half value of T_c of Hg1201 even at the optimal oxygen concentration. Although the $3d_{x^2-y^2}$ band, the Fermi surface, and its Wannier-orbitals are similar for these superconductors, there is an apparent difference in the unoccupied levels above E_F. Based on our MR-DFT, effective two-particle exchange interactions are estimated to derive enhancement in intra-layer exchange interactions for $HgBa_2CuO_4$, (Fig. 1) while it is weakened in $TlBaLaCuO_5$ and furthermore it is weak in $TlBa_2CuO_5$. The characteristic difference in the band structure is correlated with oxygen contents in the buffer layer. We also comment on the similar feature in triple-layered compounds. Our spin-fluctuation enhancement mechanism in an electron-correlation regime is consistent with the experimental fact.[3]

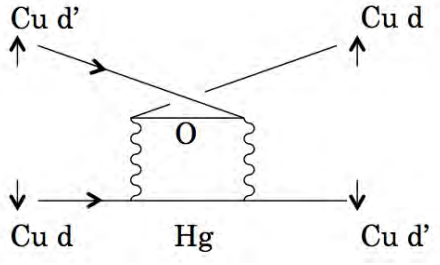

Figure 1: The super exchange mechanism giving material dependence for the layered cuprate superconductors.

Acknowledgement

The author (K.K.) is grateful to Prof. I. Maruyama, Dr. K. Nishiguchi, Mr. S. Miyao, Mr. S. Gagus Ketut, Mr. N. Morishita in physics groups, and Prof. T. Enoki, Prof. T. Mori, Prof. M. Kiguchi, Prof. K. Takai, Prof. S. Fujii, Mr. M. Ziatdinov, and Mr. Y. Kudo in chemistry groups. This work was partly supported by KAKENHI (No. 2610752, 26400357, 16HH00914).

References

[1] K. Kusakabe and I. Maruyam, J. Phys. A: Math. Theor. **44**, 135305 (2011). [2] K. Kusakabe and I. Maruyam, Japanese patent No. 5447674. [3] S. Teranishi, S. Miyao, K. Nishiguchi, K. Kusakabe, arXiv:1704.06559. [4] N. Morishita, G.K. Sunnardianto, S. Miyao, K. Kusakabe, J. Phys. Soc. Jpn., **85**, 084703 (2016). [5] S. Miyao, N. Morishita, G.K. Sunnardianto, K. Kusakabe, J. Phys. Soc. Jpn. **86**, 034802 (2017). [6] G.K. Sunnardianto, I. Maruyama, K. Kusakabe, J. Comput. Theor. Nanosci. **13**, 4883 (2016). [7] G.K. Sunnardianto, I. Maruyama, K. Kusakabe, Advanced Science, Engineering and Medicine, **8**, 421 (2016). [8] G.K. Sunnardianto, I. Maruyama, K. Kusakabe, Int. J. Hydrogen Energy (2017) in press. [9] M. Ziatdinov, H. Lim, S. Fujii, K. Kusakabe, M. Kiguchi, T. Enoki, and Y. Kim, Phys. Chem. Chem. Phys. **19**, 5145-5154 (2017). [10] K. Nishiguchi, S. Teranishi, K. Kusakabe, arXiv:1704.04867.

References

[1] K. Kusakabe and I. Maruyam, J. Phys. A: Math. Theor. **44**, 135305 (2011).

[2] K. Kusakabe and I. Maruyam, Japanese patent No. 5447674.

[3] S. Teranishi, S. Miyao, K. Nishiguchi, K. Kusakabe, arXiv:1704.06559.

[4] N. Morishita, G.K. Sunnardianto, S. Miyao, K. Kusakabe, J. Phys. Soc. Jpn., **85**, 084703 (2016).

[5] S. Miyao, N. Morishita, G.K. Sunnardianto, K. Kusakabe, J. Phys. Soc. Jpn. **86**, 034802 (2017).

[6] G.K. Sunnardianto, I. Maruyama, K. Kusakabe, J. Comput. Theor. Nanosci. **13**, 4883 (2016).

[7] G.K. Sunnardianto, I. Maruyama, K. Kusakabe, Advanced Science, Engineering and Medicine, **8**, 421 (2016).

[8] G.K. Sunnardianto, I. Maruyama, K. Kusakabe, Int. J. Hydrogen Energy (2017) in press.

[9] M. Ziatdinov, H. Lim, S. Fujii, K. Kusakabe, M. Kiguchi, T. Enoki, and Y. Kim, Phys. Chem. Chem. Phys. **19**, 5145-5154 (2017).

[10] K. Nishiguchi, S. Teranishi, K. Kusakabe, arXiv:1704.04867.

Quantum Monte Carlo simulation and electronic state calculations in correlated electron systems

Takashi YANAGISAWA
Electronics and Photonics Research Institute
National Institute of Advanced Industrial Science and Technology (AIST)
AIST Central 2, 1-1-1 Umezono, Tsukuba 305-8568

We investigated the two-dimensional Hubbard model by adopting improved wave functions that take into account intersite correlations beyond the Gutzwiller ansatz. Our wave function is an $\exp(-\lambda K)-P_G$-type wave function, which is inspired by the wave function used in quantum Monte Carlo methods. The wave function can be improved systematically by multiplying by P_G and $e^{-\lambda K}$ where K is the kinetic-energy operator.

The single-band Hubbard model is given by

$$H = \sum_{ij\sigma} t_{ij} c^{\dagger}_{i\sigma} c_{j\sigma} + U \sum_{i} n_{i\uparrow} n_{i\downarrow}, \qquad (1)$$

where t_{ij} are transfer integrals and U is the on-site Coulomb energy. The transfer integral t_{ij} is non-zero $t_{ij} = -t$ for nearest-neighbor pair $\langle ij \rangle$ and $t_{ij} = -t'$ for next-nearest neighbor $\langle\langle ij \rangle\rangle$. Otherwise t_{ij} vanishes. We denote the number of sites as N and the number of electrons as N_e. The energy unit is given by t.

The well-known Gutzwiller wave function is given by $\psi_G = P_G \psi_0$ where P_G is the Gutzwiller operator defined by $P_G = \prod_j (1-(1-g) n_{j\uparrow} n_{j\downarrow})$ with the variational parameter g in the range of $0 \le g \le 1$. The one way to improve the wave function is to take account of nearest-neighbor doublon-holon correlation: $\psi_{d-h} = P_{d-h} P_G \psi_0$. We can take into account inter-site correlations by multiplying P_J such as $P_J P_{d-h} P_G \psi_0$.

In the other way, we can take account of inter-site correlation by multiplying the kinetic operator to the Gutzwiller function in order to improve the wave function. A typical wave function of this type is written as[1]

$$\psi_\lambda \equiv \psi^{(2)} = e^{-\lambda K} P_G \psi_0, \qquad (2)$$

where K is the kinetic term in the Hamiltonian: $K = \sum_{ij\sigma} t_{ij} c^{\dagger}_{i\sigma} c_{j\sigma}$ and λ is a variational parameter to be optimized to lower the energy. This wave function is further improved by multiplying the Gutzwiller operator again:

$$\psi^{(3)} \equiv P_G \psi_\lambda = P_G e^{-\lambda K} P_G \psi_0. \qquad (3)$$

The expectation values are evaluated by using the variational Monte Carlo method.

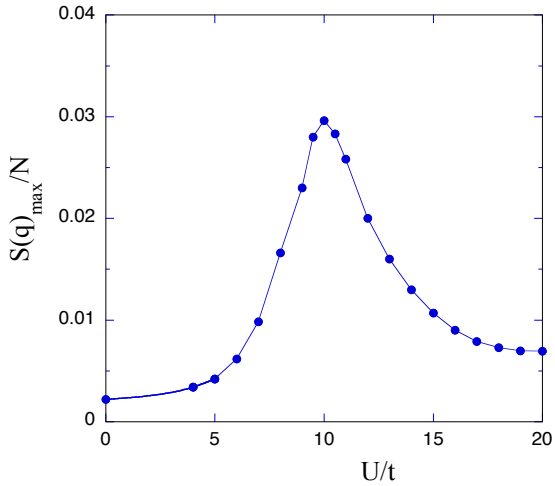

Figure 1: Spin correlation function as a function of U in units of t on 10×10 lattice. The number of electrons is $N_e = 88$ and we set $t' = 0.0$. We used the periodic boundary condition in one direction and the anti-periodic one in the other direction.

The trial wave function $P_{d-h} P_G \psi_0$ was used to develop the physics of Mott transition following the suggestion that the Mott transition occurs due to doublon-holon binding. We examined the Mott transition with the wave function $e^{-\lambda K} P_G \psi_0$[4] because the variational

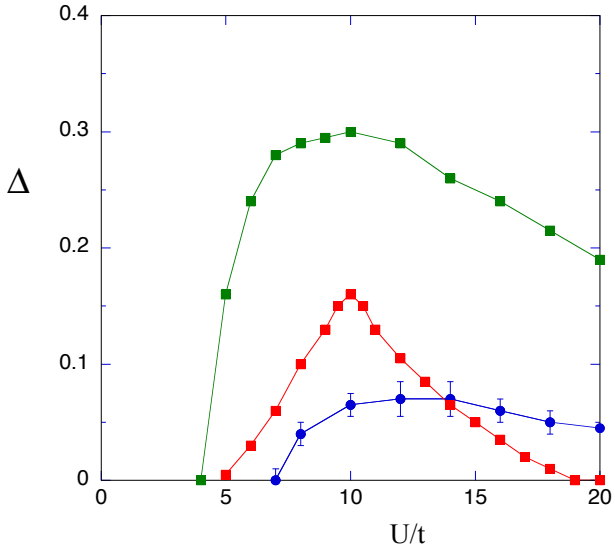

Figure 2: Superconducting and antiferromagnetic order parameters as functions of U in units of t on 10×10 lattice. The number of electrons is $N_e = 88$ and $t' = 0.0$. The solid circles show the SC gap for the improved wave function. The squares represent the antiferromagnetic order parameter, where the upper curve is for the Gutzwiller wave function and the lower curve is for the improved wave function. The boundary condition is periodic in one direction and anti-periodic in the other direction.

energy by this wave function is much lower than that of the doublon-holon wave function.

The $\mathbf{q} = (\pi, \pi)$ component of $S(\mathbf{q})$ is shown in Fig.1, where $S(\mathbf{q})$ is defined as

$$S(\mathbf{q}) = \frac{1}{N} \sum_{ij} e^{iq\cdot(r_i - r_j)} \frac{1}{4} \langle (n_{i\uparrow} - n_{i\downarrow})(n_{j\uparrow} - n_{j\downarrow}) \rangle. \tag{4}$$

$S(\mathbf{q})$ has a maximum at $\mathbf{q} = (\pi, \pi)$. The calculations were performed using the improved wave function ψ_λ. $S(\pi, \pi)$ has a peak near $U \simeq 10t$. The spin correlation is suppressed when U is extremely large begin larger than the bandwidth. There is a crossover from weakly to strongly correlated regions as U increases. The antiferromagnetic correlation induced by U is reduced for hole doping when U is large. begin greater than the bandwidth.

The optimized superconducting order parameter Δ increases as U increases, and also has a maximum at some U. We show Δ and the antiferromagnetic (AF) order parameter as functions of U in Fig.2. The superconducting correlation is developed in the region where the AF correlation is suppressed. The reduction of the antiferromagnetic correlation the strongly correlated region suggests the existence of a large antiferromagnetic spin fluctuation. The development of a superconducting correlation is understood to be induced by spin and charge fluctuations that are induced by the process to gain the kinetic energy. The charge fluctuation induced by the kinetic operator is appreciable and helps electrons to form pairs. The spin fluctuation in the strongly correlated region should be distinguished from that in a weakly correlated region. The latter is the conventional spin fluctuation.

The improved wave function gives results that are qualitatively different from those obtained by the simple Gutzwiller function. In particular, the picture of the stability of the antiferromagnetic state is crucially changed when we employ wave functions with intersite correlations.

References

[1] T. Yanagisawa et al., J. Phys. Soc. Jpn. 67, 3867 (1998).

[2] T. Yanagisawa, Phys. Rev. B75, 224503 (2007) (arXiv: 0707.1929).

[3] T. Yanagisawa, New J. Phys. 15, 033012 (2013).

[4] T. Yanagisawa and M. Miyazaki, EPL 107, 27004 (2014).

[5] T. Yanagisawa, J. Phys. Soc. Jpn. 85, 114707 (2016).

[6] I. Hase, T. Yanagisawa and K. Kawashima, Nanoscale Research Letters 12, 127 (2017).

[7] T. Yanagisawa, I. Hase and K. Odagiri, Phys. Lett. A381, 737 (2017).

Study of skyrmion in frustrated magnets with inversion symmetry

Satoru Hayami
Department of Physics, Hokkaido University, Sapporo, 060-0810

Noncollinear and noncoplanar magnetic structures including skyrmions and vortices act as emergent electromagnetic fields and lead to novel electronic and transport properties. Recently, theoretical studies have shown that such noncoplanar multiple-Q orderings are realized in the ground state in spin-charge coupled systems, such as the Kondo lattice model [1, 2]. The instability toward these magnetic orderings originates from higher-order multiple spin interactions beyond the Ruderman-Kittel-Kasuya-Yosida (RKKY) interaction, which appears after tracing out the itinerant electron degree of freedom. The interplay between charge and spin degrees of freedom, however, results in a variety of multiple spin interactions and its analysis becomes more complicated in the higher-order terms. Thus, it is crucial to elucidate essential contributions among effective magnetic interactions in itinerant magnets and construct a fundamental effective model for further exploration of exotic magnetic orderings.

In this project, in order to clarify the minimal ingredient to capture the essential physics in itinerant magnets, we derive a minimal effective spin model. First, we begin with a Kondo lattice model consisting of itinerant electrons and localized spins on square and triangular lattices, which is given by

$$\mathcal{H} = -\sum_{i,j,\sigma} t_{ij} c^{\dagger}_{i\sigma} c_{j\sigma} + J \sum_{i,\sigma,\sigma'} c^{\dagger}_{i\sigma} \boldsymbol{\sigma}_{\sigma\sigma'} c_{i\sigma'} \cdot \mathbf{S}_i, \quad (1)$$

where $c^{\dagger}_{i\sigma}$ ($c_{i\sigma}$) is a creation (annihilation) operator of an itinerant electron at site i and spin σ. In the first term, we consider hopping elements between nearest-neighbor sites, $t_{ij} = t_1$, and third-neighbor sites, $t_{ij} = t_3$, although qualitative features derived from the model in Eq. (1) are expected to hold for other choices of the hopping elements, e.g., second-neighbor hopping instead of t_3, whenever the bare magnetic susceptibility shows multiple maxima at symmetry-related wave numbers. In the second term, $\boldsymbol{\sigma} = (\sigma^x, \sigma^y, \sigma^z)$ is the vector of Pauli matrices, $\mathbf{S}_i$ is a localized spin at site i which is regarded as a classical spin with length $|\mathbf{S}_i| = 1$, and J is the exchange coupling constant.

Carefully examining the higher-order perturbations in terms of the spin-charge coupling J in Eq. (1), we have obtained an effective spin model composed of the bilinear and biquadratic interactions with particular wave numbers dictated by the Fermi surface as follows [3]:

$$\mathcal{H} = 2\sum_{\nu} \left[-\tilde{J} \mathbf{S}_{\mathbf{Q}_\nu} \cdot \mathbf{S}_{-\mathbf{Q}_\nu} + \tilde{K} (\mathbf{S}_{\mathbf{Q}_\nu} \cdot \mathbf{S}_{-\mathbf{Q}_\nu})^2 \right], \quad (2)$$

where the sum is taken for $\nu = 1, 2$ $(1, 2, 3)$ for the square (triangular) lattice, and $\mathbf{Q}_\nu$ are the wave numbers for the multiple peaks of the bare susceptibility; $\tilde{J}$ and $\tilde{K}$ are the coupling constants for bilinear and biquadratic interactions in momentum space, which originate from the RKKY interaction ($\propto J^2$) and higher-order interaction ($\propto J^4$), respectively.

By performing the Monte Carlo simulation for the model in Eq. (2), we have shown that our model provides a unified understanding of unconventional multiple-Q magnetic orders previously found in the Kondo lattice

model in Eq. (1) [1, 2]. Moreover, by applying an external magnetic field to our effective model, we have found a variety of field-induced multiple-Q phases including different types of double(triple)-Q states on the square (triangular) lattice. Our findings will serve as a guide for exploring further exotic magnetic orderings in itinerant magnets.

References

[1] R. Ozawa, S. Hayami, K. Barros, G.-W. Chern, Y. Motome, and C. D. Batista, J. Phys. Soc. Jpn. **85**, 103703 (2016).

[2] R. Ozawa, S. Hayami, and Y. Motome, Phys. Rev. Lett. **118**, 147205 (2017).

[3] S. Hayami, R. Ozawa, and Y. Motome, preprint (arXiv: 1703.07690).

Numerical analysis on a transverse-field Ising Kondo lattice model

Kazumasa HATTORI, Kohei SUZUKI

Department of Physics, Tokyo Metropolitan University,

1-1 Minami-osawa, Hachioji, Tokyo 192-0397, Japan

Ferromagnetic superconductors have attracted great attentions in condensed matter physics both in theory and experiments in the last decade. Uranium-based heavy-fermion compounds such as UGe_2, URhGe, and UCoGe show unconventional superconductivity within their ferromagnetic phases and show very interesting behaviors in magnetic fields [1]. A special attention in our work is paid to the existence of the second superconducting dome in URhGe under the transverse magnetic field (against the Ising axis of the ferromagnetism). We have analyzed one-dimensional Kondo lattice model with a single-ion anisotropy and transverse magnetic field by means of the density matrix renormalization group.

In order to speed up the calculations, we have utilized the spin-parity eigenvalue that remains even in our very anisotropic Kondo lattice Hamiltonian under transverse fields. Using the eigenstates, we can block-diagonalize the full Hamiltonian and also the density matrix. We find several phases under the transverse fields such as a ferromagnetic, antiferromagnetic, Tomonaga-Luttinger liquids (TLL), gapped Kondo-plateau, charge-density wave, and fully polarized states. The ferromagnetic state appears for lower filling and larger Kondo coupling J regime, while the gapped Kondo-plateau state appears in a wide range of the electron filling for large J. The TLL appears in a broad range of the transverse field strength between the ordered (or the Kondo-plateau) states and fully-polarized state.

To understand the connections between the ferromagnetism and superconductivity in the U-based superconductors, we will need further analyses of the various phase boundaries appearing in the phase diagram and achieve much higher precision for the analysis about the superconducting correlation functions.

References

[1] See, a recent review: D. Aoki and J. Flouquet, J. Phys. Soc. Jpn. **81**, 011003 (2012).

Electronic structure calculations of strongly correlated Ce compounds using the dynamical mean-field theory

Junya OTSUKI
Department of Physics, Tohoku University, Sendai 980-8578

4f electrons in rare-earth ions behaves as a localized moment and/or an itinerant electron depending on materials and situations. First-principles calculations based on density functional theory (DFT) give descriptions of *either* localized or itinerant state. Interesting phenomena such as heavy fermions and exotic superconductivities, however, emerge in the intermediate regime, where 4f electrons show *dual* itinerant and localized characters. In its descriptions, inclusion of many-body effects is essential. For this purpose, we perform dynamical mean-field theory (DMFT) calculations on the top of DFT results.

Here, we give a brief descriptions of our computation scheme and a setup on the ISSP supercomputer. The calculation scheme is summarized in Fig. 1. We first perform DFT calculations within LDA/GGA using `WIEN2k` package on a local computer. The Bloch states are projected to Wannier orbitals to define an effective lattice Hamiltonian using `DFTTools` [1] of `TRIQS` library [2]. Thus obtained Hamiltonian parameters and information of the material are transfered to the supercomputer and plugged into DMFT calculations. Within DMFT, the local correlation effect is evaluated through an effective Anderson impurity model, which is solved by continuous-time quantum Monte Carlo method [3] in `ALPSCore` implementation [4]. This calculation is repeated until convergence is reached. All the above packages are compiled in `C++14` mode of `gcc` version 5.1.0 to keep compatibility with the

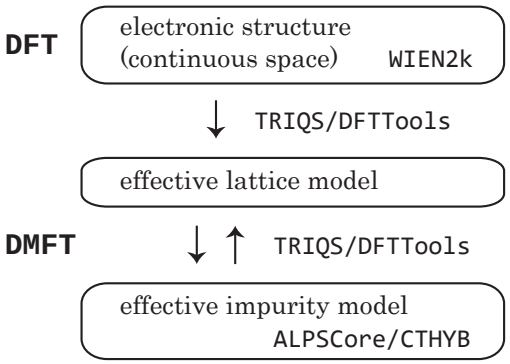

Figure 1: A flow chart of the DFT+DMFT scheme and softwares used in each step.

`TRIQS`-based softwares, which are written with the `C++14` standard.

We have done test calculations of the DMFT loop. Low-temperature calculations of order 100K are expected for Ce-based compounds. Further computations are necessary to obtain results that can be compared with experiments.

References

[1] M. Aichhorn *et al.*, Comp. Phys. Comm. **204**, 200 (2016).

[2] O. Parcollet *et al.*, Comp. Phys. Comm. **196**, 398 (2015).

[3] E. Gull *et al.*, Rev. Mod. Phys. **83**, 349 (2011).

[4] H. Shinaoka, E. Gull, P, Werner Comp. Phys. Commun. **215**, 128 (2017).

Microscopic theory for magnons of chiral magnets

Naoya ARAKAWA

Center for Emergent Matter Science, RIKEN, Wako, Saitama 351-0198

Magnons are quasiparticles describing low-energy physics of magnets. The understanding for nonchiral magnets, such as ferromagnets and antiferromagnets, has been developed. In contrast to the understanding for nonchiral magnets, the understanding for chiral magnets is developing; chiral magnets are magnets having the finite spin scalar chirality. In particular, it is unclear about the differences between magnons of nonchiral and chiral magnets and the differences between magnons of different chiral magnets.

To advance the understanding for chiral magnets, we studied the magnon dispersion and specific heat for chiral magnets on the pyrochlore lattice [1]. This study was done by using the linearized-spin-wave approximation for an effective model of pyrochlore magnets for the weak spin-orbit coupling; the effective model consists of the Heisenberg interactions and the Dzyaloshinsky-Moriya interactions. As the chiral magnets, we considered the all-in/all-out (AIAO) type chiral magnets and the three-in-one-out (3I1O) type chiral magnets.

There are two main results. First, we show that in all the chiral magnets considered, there is no gapless excitation in the magnon dispersion curves. Since a gapless excitation exists in nonchiral magnets, this result demonstrates that the absence and presence of the gapless excitations is the difference between magnons of chiral and nonchiral magnets. Second, we show that magnons for the 3I1O type chiral magnets possess not only the quasiacoustic branches of the magnon dispersion but also the optical branch, while the branches for the AIAO type chiral magnets are all quasiacoustic. Here a quasiacoustic branch increases with the displacement from $\boldsymbol{q}=\boldsymbol{Q}$, with the ordering vector $\boldsymbol{Q}$, and an optical branch decreases with the displacement. The above difference demonstrates the difference between magnons of different chiral magnets.

The facilities of the Super Computer Center were useful because the pyrochlore magnets offer the systematic numerical calculations to study the magnon properties due to the complex structure. We thus acknowledge support from the Super Computer Center.

References

[1] N. Arakawa: Magnon dispersion and specific heat of chiral magnets on the pyrochlore lattice, submitted to PRB.

Intradimer charge degree of freedom, magnetism, and superconductivity in κ-type molecular conductor

Hiroshi WATANABE
Waseda Institute for Advanced Study, Waseda University
1-6-1 Nishi Waseda, Shinjuku-ku, Tokyo 169-8050

The family of quasi two-dimensional molecular conductors κ-(BEDT-TTF)$_2$X has been extensively studied as a typical example of strongly correlated electron system. Due to the strong hybridization, two BEDT-TTF molecules facing each other can be regarded as a dimer and form an anisotropic triangular lattice with one hole per dimer (effective 1/2-filled system). Depending on the monovalent anion X, they show various quantum phases such as antiferromagnetic and spin-liquid dimer-Mott insulators, and superconductivity (SC) [1]. Owing to the similarities in the experimental phase diagrams, κ-(BEDT-TTF)$_2$X system is often compared with high-T_c copper oxides, which exhibit Mott metal-insulator transition and SC [2]. One of the theoretical models common to them is the two-dimensional Hubbard model, and the 1/2-filled case has been heavily studied. Early works suggested SC near the Mott insulating phases, but some of the recent numerical works do not support such results, and cast doubt on the simple "Mott" picture believed in κ-(BEDT-TTF)$_2$X for years.

Although the effective 1/2-filled dimer model well describes the Mott physics, recent experimental and theoretical studies suggest the importance of intradimer charge degree of freedom which are neglected in the dimer model. The intradimer charge degree of freedom leads to charge fluctuations within the dimers and should affect the electronic structure and mechanisms of emergent phenomena. Here, we theoretically study the phase competition in κ-(BEDT-TTF)$_2$X by taking account the intradimer charge degree of freedom. We consider a 3/4-filled four-band extended Hubbard model including onsite (U) and intersite Coulomb interactions (V_{ij}) with κ-type geometry with the largest hopping integral t_{b_1} as an energy unit. The ground state properties are studied with the variational Monte Carlo (VMC) method. The Gutzwiller-Jastrow type wave function is used for the VMC trial wave function. The system sizes for calculation are from 288 (4×12×6) to 1152 (4×24×12).

In the ground state phase diagram of the model parameters for X=Cu[N(CN)$_2$]Br, we find the SC state near the border between the dimer-Mott and charge-ordered states (Fig. 1) [3]. The extended-s+$d_{x^2-y^2}$-wave symmetry is favored and the gap function changes its sign depending on the band [4, 5]. Without the intersite Coulomb interactions, SC is difficult to arise since not only the spin fluctuation but also the charge fluctuation is important for the stability of SC. Our result supports the importance of intradimer charge degree of freedom and leads to a unified view of κ-(BEDT-TTF)$_2$X.

References

[1] K. Kanoda: J. Phys. Soc. Jpn. **75** (2006) 051007.

[2] R. H. McKenzie: Science **278** (1997) 820.

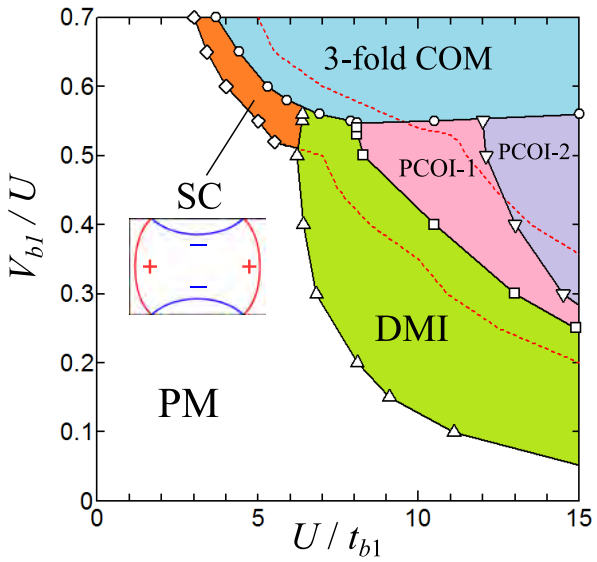

Figure 1: Ground-state phase diagram of the 3/4-filled extended Hubbard model for κ-(BEDT-TTF)$_2$X. PM, DMI, PCOI, 3-fold COM, SC denote paramagnetic metal, dimer-Mott insulator, polar charge-ordered insulator, 3-fold charge-ordered metal, and superconductivity, respectively.

[3] H. Watanabe, H. Seo, and S. Yunoki: J. Phys. Soc. Jpn. **86** (2017) 033703.

[4] K. Kuroki, T. Kimura, R. Arita, Y. Tanaka, and Y. Matsuda: Phys. Rev. B **65** (2002) 100516(R).

[5] D. Guterding, M. Altmeyer, H. O. Jeschke, and R. Valentí, Phys. Rev. B **94** (2016) 024515.